0026-895X/91/050679-11$03.00/0

MOLECULAR PHARMACOLOGY, 39:679-689

Characterization of Multiple [^{3}H]Ryanodine Binding Sites on the Ca^{2+} Release Channel of Sarcoplasmic Reticulum from Skeletal and Cardiac Muscle: Evidence for a Sequential Mechanism in Ryanodine Action

ISAAC N. PESSAH and ILDIKO ZIMANYI[1]

Department of Veterinary Pharmacology and Toxicology, University of California, Davis, California 95616

Received August 13, 1990; Accepted February 22, 1991

SUMMARY

Kinetic and equilibrium measurements of [^{3}H]ryanodine binding to the Ca^{2+} release channel of rabbit skeletal and rat cardiac sarcoplasmic reticulum (SR) are examined to ascertain the nature of cooperative interactions among high and low affinity binding sites and to quantitate their distribution. Equilibrium studies reveal affinities of 1–4 nM for the highest affinity binding site and of 30–50 nM, 500–800 nM, and 2–4 μM for the lower affinity sites in both preparations, with Hill coefficients of significantly <1, and initial rates of association and dissociation increase with increasing concentrations of ryanodine. SR vesicles are actively loaded in the presence of pyrophosphate, and fluctuations in extravesicular Ca^{2+} are measured by the absorbance change of antipyrylazo III. The data demonstrate a biphasic, time- and concentration-dependent action of ryanodine on the release of Ca^{2+}, with an initial activation and a subsequent inactivation phase. Kinetic analysis of the activation of Ca^{2+} release by ryanodine, in consonance with the binding data, demonstrates the existence of multiple binding sites for the alkaloid on the channel complex, with nanomolar to micromolar affinities. Based on the present findings obtained by receptor binding analysis and Ca^{2+} transport measurements, we suggest a model that describes four, most plausibly negatively cooperative, binding sites on the Ca^{2+} release channel. Occupation of ryanodine binding sites produces sequential activation followed by inactivation of the SR channel, revealing the strong possibility of an irreversible uncoupling of the native function of the receptor/channel complex by high concentrations of ryanodine. A model relating ryanodine receptor occupancy with SR Ca^{2+} release stresses two important new findings regarding the interaction of ryanodine with its receptor. First, ryanodine binds to four sites on the oligomeric channel complex with decreasing affinities, which can be best described by allosteric negative cooperativity. Second, binding of ryanodine to its receptor activates the Ca^{2+} release channel in a concentration-dependent and saturable manner in the range of 20 nM to 1 mM and produces a kinetically limited and sequential inactivation of the Ca^{2+} channel, with the concomitant attainment of full negative cooperativity. The results presented suggest that driving of the complex toward full negative cooperativity with high concentrations of ryanodine promotes a long-lived conformational state in which ryanodine is physically occluded and hindered from free diffusion from its binding site.

The functional aspects of the ryanodine receptor-Ca^{2+} release channel complex of SR have been extensively studied in recent years with isolated skeletal and cardiac membrane vesicles, under both passive (1–5) and active (6–9) loading conditions. Clearly, the SR channel protein comprises a number of binding domains for physiologically relevant signal molecules (e.g., Ca^{2+}, Mg^{2+}, and adenine nucleotides) and pharmacological probes (e.g., ryanodine, anthraquinones, caffeine, and ruthenium red), which can modify its gating properties and thereby alter the sensitivity of the channel to changing T tubule membrane potential (10–13). There is general agreement that the plant alkaloid ryanodine specifically binds to the SR Ca^{2+} release channel and markedly changes the Ca^{2+} transport properties of SR in a complex manner. At low concentrations ranging from 10 nM to 10 μM, ryanodine apparently causes activation of the Ca^{2+} release channel, which is characterized by a slow onset, whereas, at concentrations greater than 10 μM, ryanodine appears to inhibit channel activation (14). Both the potency and the qualitative change in SR permeability induced

This work was supported by Grant ES 05002 from the National Institute of Health and a Grant-In-Aid from the American Heart Association, California Affiliate to I.N.P.

[1] On leave from the Institute of Experimental Medicine of the Hungarian Academy of Sciences, P.O. Box 67, Budapest, H-1450, Hungary.

ABBREVIATIONS: SR, sarcoplasmic reticulum; EC_{50}, concentration of compound resulting in 50% of maximal activation; HEPES, *N*-2-hydroxyethylpiperazine-*N'*-2-ethanesulfonic acid; IC_{50}, concentration of compound resulting in 50% of maximal inhibition; mAU, milli-absorbance unit; MOPS, 3-(*N*-morpholino)propanesulfonic acid.

by ryanodine are greatly influenced by the ligands that inherently alter channel function (4). This is not surprising, because the binding of [^{3}H]ryanodine to its high affinity sites on the channel complex is highly sensitive to the same ligands that modulate SR channel activation/inactivation (15–18). The exact mechanism by which ryanodine produces its heterogeneous effects on SR permeability to Ca^{2+} remains controversial. Reconstituted SR channels in planar bilayer preparations have revealed that ryanodine concentrations of ≥10 μM are required to lock the channel in a persistent subconductance state (the apparent consequence of ryanodine binding to "high affinity" sites), whereas concentrations in excess of 1 mM are needed to completely block single-channel activity (the apparent consequence of ryanodine binding to "low affinity" sites) (14, 19). The quantitative discrepancy between ryanodine receptor binding and the ability of the alkaloid to influence the gating of the purified channel in an artificial bilayer has been attributed to its slow association kinetics. Mechanistically, the coupling between ryanodine receptor occupancy and channel function remains unclear. The important question concerning the cooperative nature among ryanodine receptor sites and the mechanism responsible for coupling of ryanodine receptor occupancy and modification of channel function has not been addressed in detail. [^{3}H]Ryanodine binding studies have shown the presence of multiple classes of specific interacting binding sites for [^{3}H]ryanodine on the skeletal and cardiac receptor protein complex. Initial reports have suggested that skeletal SR membranes comprise a single class of high affinity (having nanomolar K_d) noninteracting [^{3}H]ryanodine binding sites, whereas cardiac SR membranes exhibit high and low (K_d, ~30–400 nM) affinity sites (15, 20, 21). More recently, [^{3}H]ryanodine binding sites having very low affinity (K_d, ~3–5 μM) have been detected in both skeletal and cardiac SR, when assayed under high salt conditions (1 M KCl or NaCl) (14, 22). McGrew *et al.* (22) have suggested that positive cooperativity among binding sites may explain the slow dissociation of [^{3}H]ryanodine observed by Pessah *et al.* (17) when an excess of unlabeled ryanodine is added to the equilibrium complex. Lai *et al.* (14) have demonstrated that [^{3}H]ryanodine binding sites having low affinity show a strong tendency for negative cooperativity.

This paper characterizes in detail the kinetic and equilibrium binding interaction of [^{3}H]ryanodine with its receptor sites in SR membranes from rabbit skeletal and rat ventricle muscle, to ascertain the nature of cooperative interactions among binding sites and to quantitate the distribution among high and low affinity sites, and utilizes the method developed by Palade (7) to correlate Ca^{2+} transport across SR membrane vesicles under active loading conditions and in the presence of pyrophosphate, to directly address the relationship between ryanodine receptor occupancy and Ca^{2+} channel function. Our findings strongly suggest 1) that multiple binding sites for ryanodine (possibly four) exist on the channel protein, 2) that the binding of ryanodine among these sites can be best described by allosteric negative cooperativity, and 3) that ryanodine receptor occupancy is coupled to the Ca^{2+} release channel by a sequential, time- and concentration-dependent, activation/inactivation mechanism.

Materials and Methods

Preparation of SR membranes. Junctional SR membranes from rabbit back (fast) skeletal muscle were isolated by the method of Saito *et al.* (23). Junctional SR vesicles were rehomogenized in 0.3 M sucrose, 5 mM imidazole buffer, pH 7.4, at approximately 3 mg/ml protein, and aliquots were rapidly frozen in liquid N_2.

SR membrane vesicles from rat heart ventricles enriched in ryanodine receptor were isolated by sucrose density gradient centrifugation, as previously described (24), whereas Ca^{2+} transport measurements were performed with a cruder preparation (25) having higher ATPase activity, which facilitated Ca^{2+} loading (24). Protein concentrations were determined by the method of Lowry *et al.* (26), after removal of HEPES buffer by precipitation of protein with 2% perchloric acid, centrifugation at 30,000 × *g*, and dissolving of the pellet in 1 M NaOH.

Spectrophotometric determination of Ca^{2+} release. Ca^{2+} loading of SR vesicles and subsequent release of intravesicular Ca^{2+} were measured by a slight modification of the method of Palade (7), which utilizes pyrophosphate as a precipitating anion. Skeletal or cardiac SR membrane vesicles (50–80 μg of protein, ~20 μl) were placed in a cuvette, thermostated at 37°, containing 980 μl of 95 mM KCl, 20 mM K-MOPS, 7.5 mM sodium pyrophosphate, 250 μM antipyrylazo III, 1.5 mM MgATP, 25 μg/ml creatine phosphokinase, 5 mM phosphocreatine, pH 7.0 (final volume, 1 ml). The mixture was allowed to equilibrate for 1 min with constant stirring. Changes in the free Ca^{2+} concentration were monitored by measurement of the absorbance of antipyrylazo III at 710 nm and subtraction of the absorbance at 790 nm, at 1-sec intervals, using a diode array spectrophotometer (model 8452A; Hewlett Packard, Palo Alto, CA). In some experiments, three reactions were monitored at 4.5-sec intervals by utilizing the automated multicell transporter. The subtracted functional wavelengths, in mAU, were displayed throughout the experiment in "real time" on a monitor and concurrently stored by computer (model 9000/300; Hewlett Packard) for subsequent analysis. The vesicles were actively filled by consecutive additions of 10 or 20 nmol of $CaCl_2$, using a Hamilton syringe, by allowing the absorbance to return to the baseline between additions. All the release experiments were performed at loading levels near the respective filling capacities of skeletal (capacity = 2.2 ± 0.9 μmol of total Ca^{2+}/mg of protein) and cardiac (capacity = 1.1 ± 0.5 μmol of total Ca^{2+}/mg of protein; mean ± standard deviation of four preparations) SR preparations; levels were kept constant within a dose-response titration. The total amount of Ca^{2+} loaded into the vesicles was quantified in two ways, first, by summing of the downward deflections of absorbance in the loading phase of the experiment and, second, by the addition of 2 μg of the ionophore A23187 at the end of each experiment. The two methods were in excellent quantitative agreement (i.e., all of the Ca^{2+} loaded into the vesicles during the loading phase was released by addition of ionophore). Because the rate of Ca^{2+} release was dependent on the extravesicular free Ca^{2+} concentration, ryanodine-enhanced Ca^{2+} release was always initiated with the same level of free Ca^{2+} (as measured by absorbance) within one set of experiments, including the corresponding control. The ability of ryanodine to enhance Ca^{2+}-induced Ca^{2+} release was assessed either in the presence of a bolus of activating Ca^{2+} (drug was varied with a constant concentration of $CaCl_2$) or by the addition of the drug 30 sec after initiation of Ca^{2+}-induced release of intravesicular Ca^{2+}.

Analysis of transport data. The absorbance signals were calibrated by addition of known amounts of $CaCl_2$, from a National Bureau of Standard stock, to the complete transport mixture, in the presence of 2 μg/ml A23187 to prevent Ca^{2+} accumulation. The functional absorbance of the dye (A_{710}–A_{790}) was a linear function of the added $CaCl_2$ in the range of 10–100 μM, yielding least squares correlation coefficients of >0.99, and was stable during the course of the experiments (not shown); hence, it can be directly correlated to free Ca^{2+} outside the vesicles. The initial (fast) rates of release of accumulated Ca^{2+} were analyzed by measurement of the change in mAU/sec, using the least squares best linear fit to the steepest slope, with the Kinetics Software Program (Hewlett Packard). Rates of Ca^{2+} release were reported as mAU/mg/sec or as relative release rates. Dose-response relationships were analyzed by the nonlinear curve-fitting program ENZFITTER (Elsevier Biosoft, Cambridge, UK). The component of

Ca^{2+} release directly attributable to the presence of ryanodine was determined by subtracting the rate of Ca^{2+} release attributable to the presence of activator Ca^{2+}, at each of the respective concentrations.

Measurement of [^{3}H]ryanodine equilibrium binding. Specific binding of [^{3}H]ryanodine to skeletal and cardiac preparations was measured under identical conditions by the procedure developed by Pessah *et al.* (15). Briefly, SR vesicles (30–40 μg) were incubated in duplicate at 37° for 2 (cardiac) or 3 (skeletal) hr, with 0.5–400 nM (sites 1 and 2), 50–5,000 nM (sites 3 and 4), or 300–10,000 nM (site 4 only) [^{3}H]ryanodine, in a final volume of 1 ml of 250 mM KCl, 15 mM NaCl, 50 μM $CaCl_2$, 20 mM HEPES, pH 7.1. The assays were terminated by filtration through Whatman GF/B glass fiber filters, using a Brandel (Gaithersberg, MD) cell harvester, and were washed twice with 2.5 ml of ice-cold wash medium, consisting of 20 mM Tris·HCl, 250 mM KCl, 15 mM NaCl, and 50 μM $CaCl_2$, pH 7.1. Radioactivity was measured by scintillation counting, with an efficiency of approximately 43%. In all cases, nonspecific binding of [^{3}H]ryanodine was defined with addition of a 100-fold excess of unlabeled ryanodine. The average value of nonspecific binding to the high affinity site amounted to 5–10% of the total binding of 1 nM [^{3}H]ryanodine. The average value of nonspecific binding to the low affinity site amounted to 8–15% of the total binding of 50 nM [^{3}H]ryanodine and 25% of the total binding of 1 μM [^{3}H] ryanodine. Filter binding of [^{3}H]ryanodine in the absence of vesicular preparation was negligible.

Measurement of association/dissociation kinetics. The rate of association of [^{3}H]ryanodine binding was measured by quenching of the reaction by rapid filtration at times ranging from 2 to 360 min after the addition of SR vesicles. Dissociation of [^{3}H]ryanodine from the receptor equilibrium complex was determined by equilibration of 1 or 50 nM or 1 μM [^{3}H]ryanodine with membranes for 3 or 2 hr, for skeletal and cardiac SR, respectively, at 37°, followed by addition of a 100-fold excess of assay medium or an excess of unlabeled ryanodine or ruthenium red to the incubation mixture, and determination of residual specific binding at subsequent times ranging from 10 min to 5 hr.

Analysis of binding data. Equilibrium binding data from saturation analysis were fitted to a one- or two-site model, and the dissociation constants (K_d), maximal binding capacities (B_{max}), and Hill coefficients (n_H) were determined by nonlinear regression analysis, using the LIGAND computer program. The first-order association rate constants (k_{+1}) were calculated as described by Bennett (27), based on the apparent association rate constant (k_{obs}), which was determined by the ENZFITTER computer program, and the dissociation rate constants (k_{-1}), which were calculated by least squares linear regression analysis from $\ln(SB/SB_o) = k_{-1}t$, where SB is specific binding at time t and SB_o is specific binding at time 0; if the plots were curvilinear, they were analyzed by the ENZFITTER computer program.

Materials. [^{3}H]Ryanodine (specific activity, 95 Ci/mmol; >98 purity by high performance liquid chromatography) was obtained from New England Nuclear (Wilmington, DE); unlabeled ryanodine was purified by high performance liquid chromatography (>99%) from a commercial (Penick, Tacoma, WA) mixture of ryanodine and dehydroryanodine. Antipyrylazo III was purchased from Sigma Chemical Co. (St. Louis, MO). All other chemicals were of the highest purity available.

Results

Ca^{2+}-induced Ca^{2+} release. Rabbit skeletal SR vesicles loaded with seven incremental additions of 20 nmol/ml $CaCl_2$ readily accumulate the added Ca^{2+} (2.8 μmol of total Ca^{2+}/mg of protein, if the extravesicular free Ca^{2+} is allowed drop to a low level between additions) (Fig. 1A). Once the final addition of $CaCl_2$ is fully taken up by the vesicles and the absorbance signal returns to the baseline, bolus addition of 65 nmol/ml $CaCl_2$ (Fig. 1A, *arrowhead*) induces the release of the accumulated intravesicular Ca^{2+}, with an initial rate of 3.8 mAU/mg/sec. The initial rate of Ca^{2+} release decreases with decreasing trigger Ca^{2+} (not shown) and is completely inhibited if 25 nM

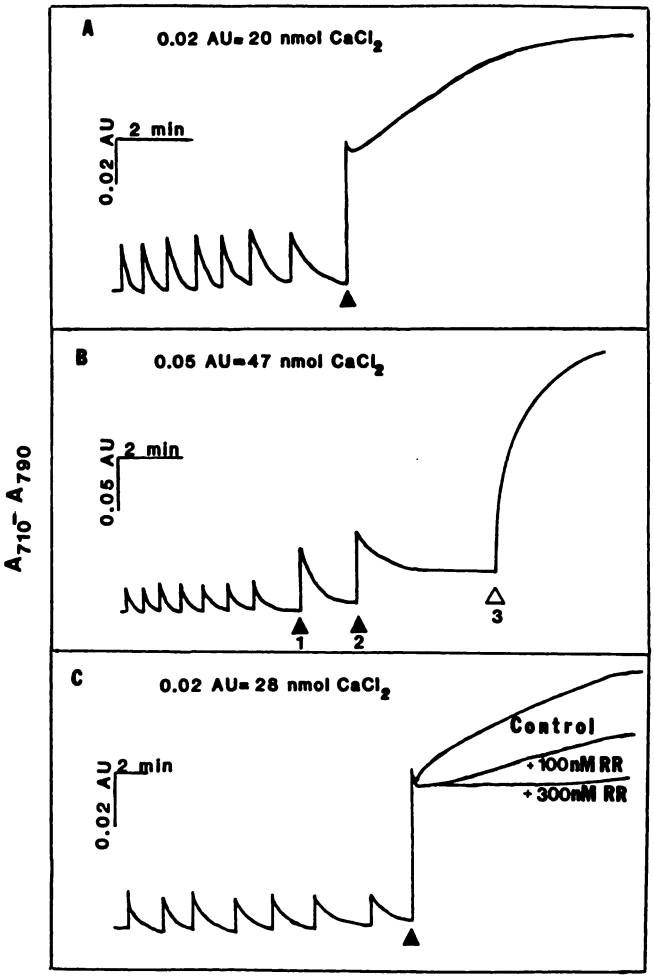

Fig. 1. Skeletal SR (50 μg) (A and B) or cardiac SR (80 μg) (C) are actively loaded with seven sequential additions of 20 μM $CaCl_2$. In A, the *arrowhead* indicates a bolus addition of 65 μM $CaCl_2$. In B, additions (*arrowheads*) are 25 nM ruthenium red plus 50 μM $CaCl_2$ (*1*), 50 μM $CaCl_2$ (*2*), and 2 μg of A23187 (*open arrowhead*) (*3*). In C, the *arrowhead* indicates addition of 50 μM $CaCl_2$ in the absence (control) and in the presence of 100 and 300 nM ruthenium red (*RR*).

ruthenium red is included with the bolus of trigger $CaCl_2$ (Fig. 1B, *first arrowhead*). A subsequent addition of 50 nmol of $CaCl_2$ fails to induce Ca^{2+} release, and the vesicles continue to actively accumulate Ca^{2+} (Fig. 1B, *second arrowhead*). Addition of 2 μg of the ionophore A23187 rapidly releases all the accumulated Ca^{2+} (Fig. 1B, *open arrowhead*). Rat ventricle preparations also exhibit Ca^{2+}-induced release of Ca^{2+} with a bolus of 50 μM Ca^{2+}, giving an initial rate of 1.1 mAU/mg/sec (Fig. 1C). The release of Ca^{2+} from cardiac preparations is less sensitive to inhibition by ruthenium red (28), although complete inhibition can be attained at higher than 100 nM concentrations (Fig. 1C).

Enhancement of Ca^{2+}-induced Ca^{2+} release by ryanodine. Ryanodine significantly enhances Ca^{2+} release from skeletal and cardiac SR, in a dose-dependent, ruthenium red-sensitive manner (Fig. 2). For example, the initial rate of Ca^{2+} release elicited by 70 μM $CaCl_2$ (optimal for ryanodine receptor binding) is 0.8 ± 0.2 mAU/mg/sec (mean ± standard deviation of 15 determinations). The threshold concentration of ryanodine required to significantly enhance the initial rate of Ca^{2+} release ranges between 10 and 25 nM in eight determinations with skeletal preparations (1.4 and 1.8 mAU/mg/sec at 10 and

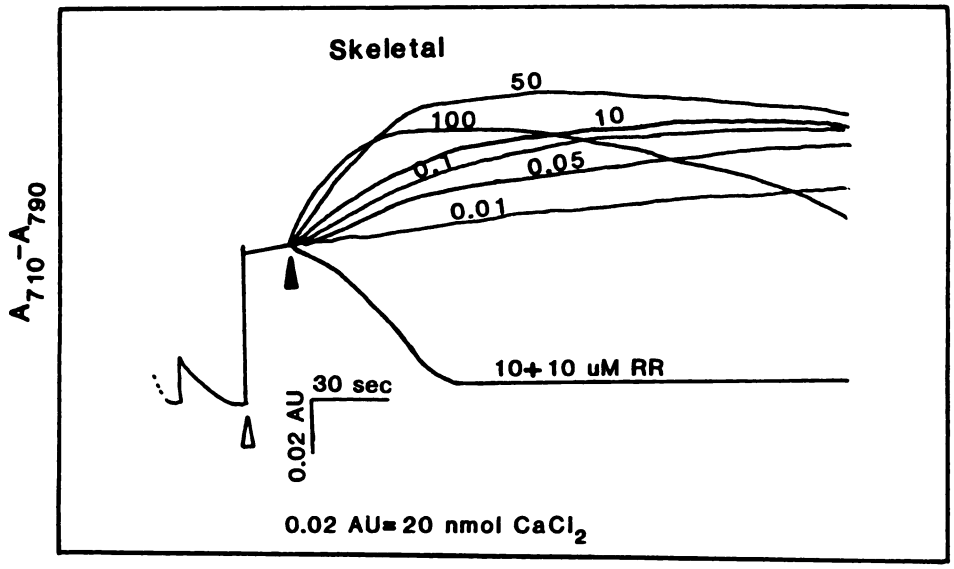

Fig. 2. Dose-dependent enhancement of the initial rate of Ca^{2+} release from skeletal SR by ryanodine. Skeletal vesicles (60 μg) are actively loaded to near their capacities, which is 0.85 ± 0.05 μmol of total Ca^{2+}/mg of protein (38 determinations). At the end of the loading phase, $CaCl_2$ (60 μM) is added (after the last bolus of $CaCl_2$ in the uptake phase, which is accumulated inside the vesicles) (*open arrowhead*), and Ca^{2+} release is allowed to proceed for approximately 25 sec. Ryanodine is added by Hamilton syringe (*arrowhead*), at concentrations indicated on the traces (μM). *RR*, ruthenium red. Each *trace* represents an individual experiment, which when uniformly scaled demonstrates the concentration-dependent influence of ryanodine on the initial rate of Ca^{2+} release.

25 nM ryanodine, respectively; *t* test significant, $p < 0.05$) (Fig. 3A). Cardiac preparations are more sensitive to Ca^{2+}-induced release of Ca^{2+} (Fig. 3A), necessitating the measurement of ryanodine-enhanced releases at lower concentrations of $CaCl_2$ (30 μM Ca^{2+} yields 2.3 ± 0.3 mAU/mg/sec). Under these conditions, the threshold concentration of ryanodine required to significantly ($p < 0.05$) enhance the initial rate of Ca^{2+} release ranges between 100 and 250 nM (eight determinations). Ryanodine (0.1–1000 μM)-enhanced release of Ca^{2+} exhibits a saturable dose-response relationship with skeletal SR and becomes saturated above 1 mM with cardiac SR (Fig. 3A). Even at 1 mM, ryanodine initially activates Ca^{2+} release maximally. The rate data for the ryanodine-induced component (after subtraction of the release rate attributable to Ca^{2+}-induced Ca^{2+} release; Fig. 3A) are transformed according to the method of Lineweaver-Burke, using only the concentrations of the alkaloid that result in 20 to 80% of the maximum Ca^{2+} release rates in the analysis. Fig. 3, B and C, demonstrates that the skeletal and cardiac release channels respond to ryanodine in a manner that deviates from simple Michaelis-Menten kinetics (i.e., con-

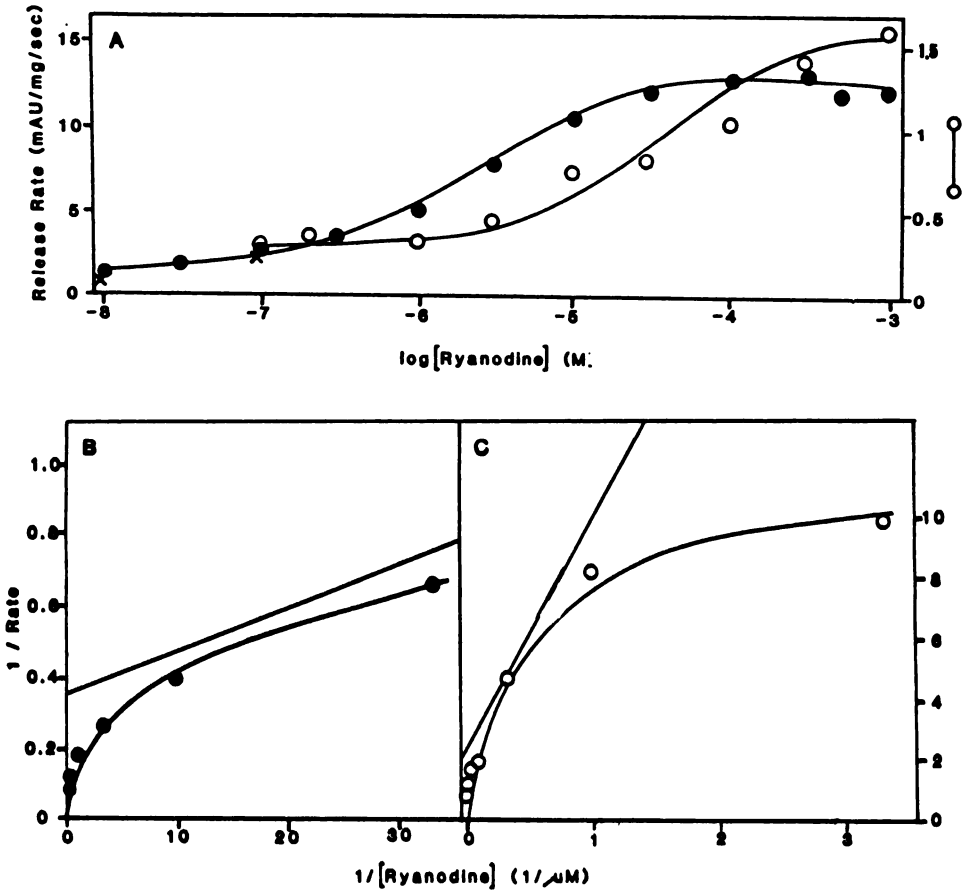

Fig. 3. Ryanodine-enhanced rapid Ca^{2+} release from cardiac (○) (80 μg) and skeletal (●) (50 μg) SR (A) actively loaded in the presence of pyrophosphate exhibits saturable dose-response curves, which are influenced by the level of activating Ca^{2+}. SR vesicles are loaded as described in Fig. 2. Release is initiated by addition of ryanodine (10 nM to 1 mM) in the presence of 30 μM Ca^{2+} (cardiac) or 70 μM Ca^{2+} (skeletal). Initial rates of Ca^{2+} release are calculated by best linear fit of the steepest component and are presented as mAU/mg/sec. ×, The component of the release rates attributable to the presence of Ca^{2+} alone. The dose-response relationships for the ryanodine-enhanced component (after subtraction of the Ca^{2+}-induced component) from skeletal and cardiac SR are transformed according to the Lineweaver-Burke method and are presented in B and C, respectively. The *lines* represent the linear fit of the plot by the ENZFITTER program.

vex Lineweaver-Burke plot) and suggests the presence of negative cooperativity with respect to the alkaloid effector sites, with Hill coefficients of 0.52 (Fig. 3B) and 0.59 (Fig. 3C). Nonlinear regression analysis of the curvilinear Lineweaver-Burke plots resolves each preparation into two components, having K_d values (mean ± standard error) of 41 ± 9 nM and 3.6 ± 0.3 μM with skeletal SR (Fig. 3B) and 0.44 ± 0.28 μM and 29 ± 10 μM with cardiac SR (Fig. 3C). The higher sensitivity of cardiac channels to Ca^{2+}-induced Ca^{2+} release precludes resolution of the higher affinity component of ryanodine-induced Ca^{2+} release that is predicted from receptor binding studies (see below). The ratio of high affinity to low affinity sites responsible for ryanodine-induced Ca^{2+} release is close to 1:3 with both preparations (maximum rates, in mAU/mg/sec, are 0.55 and 1.65 with cardiac and 3.2 and 13 with skeletal SR, respectively).

Sequential activation/inactivation of the SR release channel by ryanodine. The consequence of ryanodine binding to the SR Ca^{2+} release channel has remained unclear, because the alkaloid appears to activate the SR channel at high nanomolar to low micromolar concentrations, while inhibiting the channel at concentrations greater than 100 μM (see Introduction). We address the possibility of a sequential, kinetically limited mechanism in the coupling of ryanodine receptor binding and its consequent expression on channel activity. The experimental approach of monitoring the effects of ryanodine in real time from the moment of addition of ryanodine, under active loading conditions, allows us to directly assess the possibility of a sequential mechanism. Although Figs. 2 and 3 demonstrate that increasing ryanodine concentrations increase the initial component of release in a saturable manner (even 1 mM ryanodine produces an initial, fully activated channel), Fig. 4 shows that, pursuant to channel activation, ryanodine inactivates both the skeletal and cardiac channels, thereby allowing the reaccumulation of Ca^{2+} into the vesicles. The speed with which the inactivation phase takes place increases with increasing ryanodine, in the range of 1 μM to 1 mM, and influences the total amount of Ca^{2+} efflux in the initial release phase. Skeletal and cardiac preparations exhibit quantitative differences with respect to the dose-response relation for inactivation, suggesting that the extravesicular Ca^{2+} concentration also influences the rate of inactivation by ryanodine (Fig. 4).

High and low affinity equilibrium binding of [^{3}H]ryanodine. Scatchard analysis of equilibrium binding experiments with [^{3}H]ryanodine at optimal (50 μM) Ca^{2+} shows the presence of multiple binding sites, having nanomolar affinity, in both skeletal and cardiac SR. The Ca^{2+}-activated component (in the absence of other known chemical modulators) having the highest affinity for [^{3}H]ryanodine in skeletal and cardiac SR exhibits K_{d_1} values of 4.6 ± 1.9 nM and 1.5 ± 0.3 nM (average of three independent experiments in duplicate), respectively, regardless of whether the experiments are performed by titration of the labeled ligand at fixed specific activity (data not shown) or addition of unlabeled ligand to a fixed concentration of [^{3}H]ryanodine. The low nanomolar K_d of the high affinity site necessitates the use of 0.5–1.0 nM [^{3}H]ryanodine to demonstrate the high and the low affinity sites in the same experiment (Fig. 5). Fig. 5, *insets*, shows the high and low affinity sites measured in the presence of 0.5–32 and 15–500 nM [^{3}H]ryanodine in individual experiments. Sites having 11- and 24-fold lower affinity (K_{d_2} values) for the radioligand are present

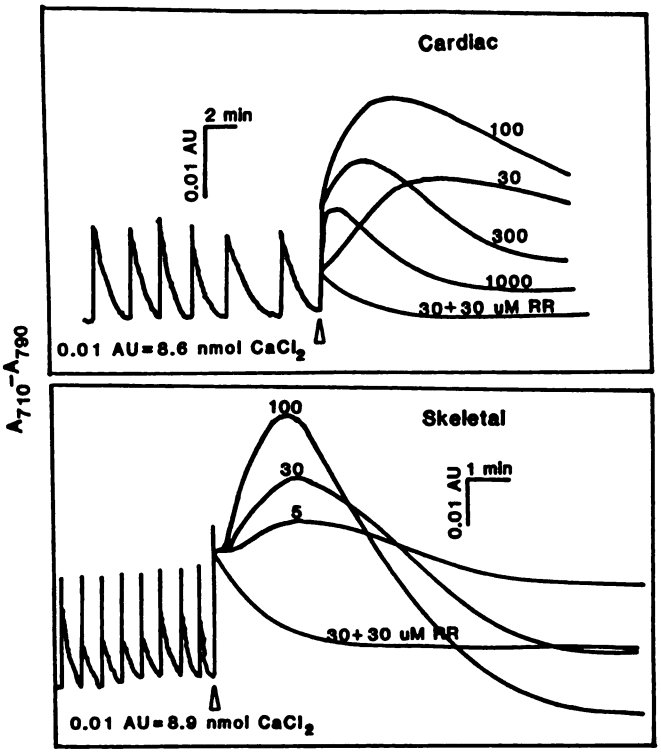

Fig. 4. Sequential activation and inactivation of the Ca^{2+} release channel of cardiac and skeletal SR. Cardiac (80 μg) and skeletal (50 μg) vesicles are loaded with 6 × 12- and 8 × 20-nmol $CaCl_2$ additions, respectively. Release is initiated with ryanodine in the presence of 5 μM $CaCl_2$ (cardiac SR) or 30 μM $CaCl_2$ (skeletal SR). Ryanodine concentrations are indicated on the traces (μM). *RR*, ruthenium red.

in skeletal and cardiac SR and are characterized by Hill coefficients significantly ($p < 0.05$) less than unity (Table 1A). The maximum receptor densities for skeletal and cardiac preparations are 23 and 7 pmol/mg of protein (best of four determinations), respectively, and are each estimated to comprise ~1:2.3 high/low affinity binding sites. Several attempts have been made to demonstrate the existence of low affinity sites having K_d values of ≥1 μM, which are reported to exist under high salt conditions (14, 22). Analysis of the binding of 50 nM [^{3}H]ryanodine in the absence and presence of 25–5000 nM unlabeled ryanodine results in binding sites having K_d (K_{d_2}) values of 554 nM in skeletal SR and 680 nM in cardiac SR and B_{max} values of 26 and 8.6 pmol/mg of protein, respectively (Table 1). Under these conditions, the corresponding n_H values are between 0.6 and 0.7 for both preparations. Analysis of experiments with 300 nM [^{3}H]ryanodine (specific activity, 4.5 Ci/mmol) and added unlabeled ryanodine from 100 nM to 10 μM, using the LIGAND computer program, repeatedly fails to compute K_d values (the regressions invariably failed to converge). However, initial estimates generated by the nonlinear Marquardt algorithm of the ENZFITTER program yield K_d (K_{d_4}) values of 2.8 μM for skeletal SR and 4.3 μM for cardiac SR, with n_H values of 0.23 and 0.27, respectively. The estimates of K_{d_4} and B_{max_4} using equilibrium ligand binding techniques have large errors associated with them, which reflect the inherent limitation of this method to ascertain K_d values of ≥1 μM. The average equilibrium K_d, B_{max}, and n_H values for the high and low affinity sites for [^{3}H]ryanodine binding are summarized in Table 1A.

Kinetic studies of high and low affinity sites. The

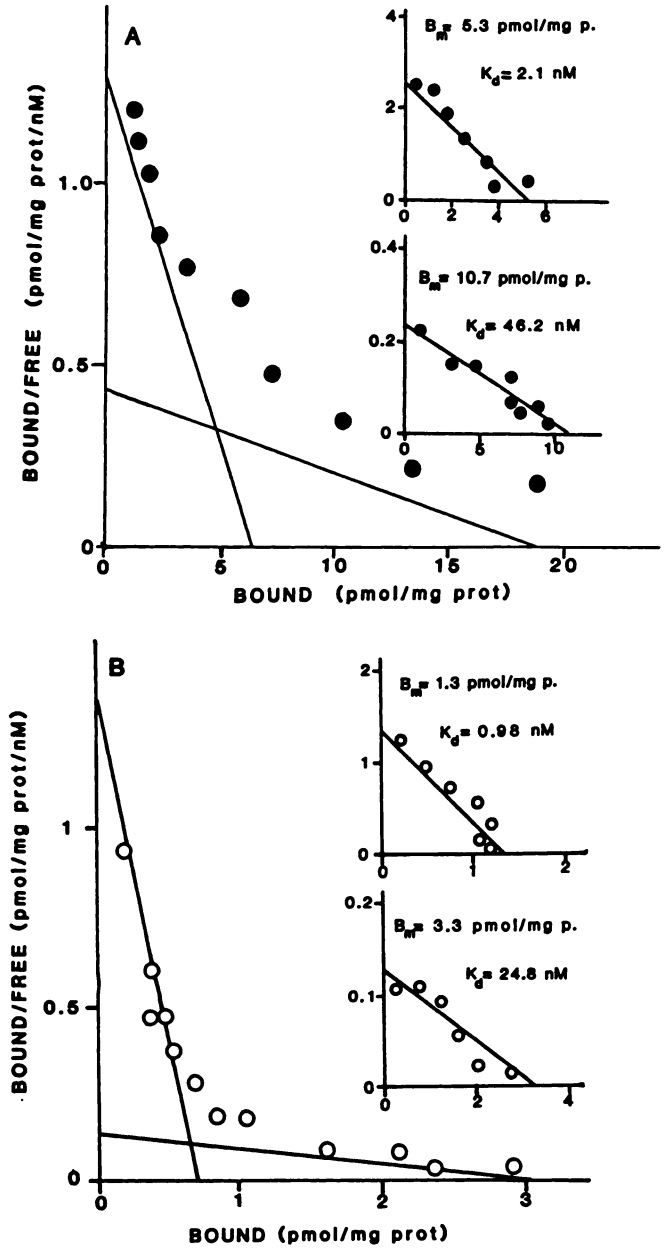

Fig. 5. Scatchard analysis of the high and low affinity binding of [^{3}H] ryanodine to 30 μg of skeletal (A) or cardiac (B) SR. Binding of [^{3}H] ryanodine (0.5–480 nM) was performed as described in Materials and Methods. A, K_d values for the high and low affinity sites are 5.22 and 44.66 nM, respectively; B_{max} values for the high and low affinity sites are 6.45 and 18.81 pmol/mg of protein, respectively. B, K_d values for the high and low affinity sites are 0.6 and 24.9 nM, respectively; B_{max} values for the high and low affinity sites are 0.84 and 3.36 pmol/mg of protein, respectively. Data shown are from representative experiments, performed in duplicate, which were repeated several times (see average constants in Table 1). *Insets*, Scatchard analysis of binding of 0.5–32 nM (*upper*) and 15–500 nM (*lower*) [^{3}H]ryanodine to skeletal (A) and cardiac (B) SR. Data shown are from single individual experiments, performed in duplicate.

association of 1 and 50 nM [^{3}H]ryanodine in cardiac and skeletal SR and of 1 μM [^{3}H]ryanodine in skeletal SR is shown in Fig. 6. The rate of association increases with the concentration of ryanodine, from 1 nM to 1 μM. Linear transformation performed on association data is shown in Fig. 7 for 1 and 50 nM [^{3}H]ryanodine at skeletal (Fig. 7A) and cardiac (Fig. 7B) SR. High [^{3}H]ryanodine concentrations (1 μM) further increase the rate of association in skeletal SR (Fig. 7A, *inset*), which is fully equilibrated in 20 min and remains stable for 6 hr.

Dissociation (induced by a 100-fold dilution of the assay medium) is shown in Fig. 6. The rate of dissociation increases with the concentration of ryanodine, from 1 to 50 nM, and the shape of the dissociation curve changes from linear to curvilinear. Dissociation rate experiments at 50 nM [^{3}H]ryanodine are indeed nonlinear with both cardiac and skeletal SR (Fig. 8). The curvilinear dissociation curves allow us to calculate the distribution of the high and low affinity sites, as well as to accurately measure their dissociation rate constants. The ENZFITTER computer program can estimate the linearized dissociation curves. The initial fast dissociation represents the low affinity site, and the slow dissociation represents the high affinity site. The ratio of these two sites can be estimated from the *y*-intercept of the slower component on the time versus $\ln(SB/SB_o)$ plot (i.e., $e^{y\text{-intercept}}$), which will give the percentage of occurrence of the high affinity site (Fig. 8). The ratio of high and low affinity sites is approximately 1:2.5 in both muscle preparations. However, the trend of increasing rates of dissociation seen with 1 and 50 nM [^{3}H]ryanodine broke, becoming slower and linear with the dissociation of 1 μM ligand-receptor equilibrium complex (Fig. 8A). This observation is not the result of reassociation of 10 nM ryanodine during measurement of dissociation of 1 μM [^{3}H]ryanodine (by 100-fold dilution), because a 2000-fold dilution under identical conditions yields a similar slow rate of dissociation (k_{-1} = 0.0028 and 0.0037 min^{-1}, respectively). By using the measured dissociation rate constants (k_{-1}) and the observed association rate constant (measured at 50 nM [^{3}H]ryanodine) (Table 1B), the K_d values for the high and low affinity sites can be calculated (Table 1C). The calculated K_d values are not significantly different from those estimated from equilibrium binding experiments, and the approximate ratio of the maximal binding capacities for the high and low affinity sites is 1:2.3. Based on the association and dissociation rate constants (Figs. 7A and 8A) at 1 μM [^{3}H]ryanodine, the calculated K_d is 4.85 nM. Please note that the equilibrium binding at 1 μM [^{3}H]ryanodine is only 11.5 pmol/mg of protein, whereas at 50 nM [^{3}H]ryanodine it is 7 pmol/mg of protein. Assuming the presence of four binding sites with the lowest affinity of 3 μM (14), the expected binding at 1 μM [^{3}H] ryanodine should be approximately 25–30 pmol/mg of protein. These data suggest that a loss of the available binding sites occurs even after 1 hr of incubation with 1 μM [^{3}H]ryanodine.

Pessah *et al.* (16, 17) have shown that the dissociation of 5 nM [^{3}H]ryanodine from its high affinity sites by a 2000-fold excess of unlabeled ryanodine has an extremely slow component of dissociation ($t_{1/2}$ = 14.4 hr), comprising 75% of all binding sites, and results in a K_d 20 times lower than the apparent K_d determined from equilibrium binding studies. To understand the basis of the discrepancy between calculated and measured K_d values for the high affinity sites, we have measured the rate of dissociation of 0.5–1.0 nM [^{3}H]ryanodine from the high affinity sites, using several concentrations of ryanodine or ruthenium red, a competitive inhibitor of the binding of ryanodine. The dissociation rate constants are listed in Table 2. The association rate constants are calculated from the k_{obs} values of 0.0148 and 0.0128 min^{-1} for cardiac and skeletal SR, respectively, according to the equations listed in the legend to Table 1. Dilution with a 100-fold excess of the assay medium or

TABLE 1

Comparison of the binding constants for [^{3}H]ryanodine binding to skeletal and cardiac SR

Values are mean ± standard error or average of two independent determinations performed in duplicate. Binding of [^{3}H]ryanodine at four concentration ranges was performed as described in Materials and Methods. 1–4 refer to the high affinity and to the lower affinity sites. $k_{+1} = (k_{obs} - k_{-1})/[L]$, where $[L]$ is the equilibrium concentration of the ligand. $K_d = k_{-1}/k_{+1}$.

A. Equilibrium experiments	K_d		B_{max}		n_H	
	Skeletal	Cardiac	Skeletal	Cardiac	Skeletal	Cardiac
	nM		pmol/mg of protein			
1	4.6 ± 1.9	1.5 ± 0.3	5.8 ± 0.2	1.5 ± 0.3	0.86 ± 0.07[a]	0.93 ± 0.07
2	52.8 ± 17.1	35.5 ± 10.7	12.9 ± 4.1	3.8 ± 0.4	0.70 ± 0.10	0.69 ± 0.10
3	554.5 ± 66.5	680.5 ± 88.4	26.1 ± 1.9	8.6 ± 2.4	0.62 ± 0.09	0.70 ± 0.08
4	2800.0 ± (>100%)	4320.0 ± (>100%)	67.2 ± (>100%)	78.7 ± (>100%)	0.23 ± 0.005	0.27 ± 0.015
					0.55 ± 0.02[b]	0.63 ± 0.04

B. Kinetic experiments[c]	k_{obs}	k_{-1_1}	k_{-1_2}	k_{+1_1}	k_{+1_2}
		min^{-1}		$nM^{-1}\ min^{-1}$	
Cardiac	0.0637	0.00212	0.0288	0.00123	0.000698
Skeletal	0.0623	0.00225	0.0292	0.00120	0.000662

C. Calculated dissociation constants	K_{d_1}	K_{d_2}
	nM	
Cardiac	1.7	41.3
Skeletal	1.9	44.1

[a] Values for n_H are mean ± standard error of three independent determinations performed at four different ranges of [^{3}H]ryanodine concentrations, as described in Materials and Methods.
[b] Hill coefficient determined from [^{3}H]ryanodine binding curve using labeled ligand concentrations only from 0.2 nM to 2 μM.
[c] Ryanodine concentration, 50 nM.

addition of 50 nM ryanodine (which is a 100-fold excess of the labeled ligand) causes rapid dissociation of [^{3}H]ryanodine from the high affinity site of both preparations. In both preparations, the off-rate of 1 nM [^{3}H]ryanodine slightly increases (cardiac SR) or does not change (skeletal SR) with the concentration of ruthenium red, from 200 nM to 1 μM (Table 2). Ryanodine (10 μM) seems to dissociate 1 nM [^{3}H]ryanodine in a biphasic manner in both preparations, with a rapid ($t_{1/2}$ = 80–100 min) and a very slow phase ($t_{1/2}$ = several hours). It is very important to point out that these experiments aim to assess the dissociation rate of ryanodine from its highest affinity site, whose initial rate does not decrease with increases in the ryanodine concentration from 25 nM to 10 μM. At a 20,000-fold concentration of unlabeled ryanodine, the appearance of a very slow, late phase of the dissociation can be due to a subsequent irreversible action of ryanodine on the lower affinity sites and is in consonance with the finding that the dissociation rate measured with a 100-fold dilution of the assay medium slows down as the concentration of the equilibrating [^{3}H]ryanodine increases from 50 nM to 1 μM.

Influence of Ca^{2+} transport buffer on [^{3}H]ryanodine binding parameters. The validity of conclusions drawn from radioligand binding and Ca^{2+} transport assays reported here hinges on the assumption that the characteristics of ryanodine binding to the channel complex are essentially the same in the antipyrylazo III transport buffer as those measured in the standard assay buffer. Binding curves performed in the complete transport buffer are essentially identical to those measured in standard assay buffer, exhibiting curvilinear Scatchard plots with similar values for K_{d_1} and K_{d_2} (Fig. 9). [^{3}H]Ryanodine binding in the transport buffer maintains its sensitivity to key ligands, including Ca^{2+}, adenine nucleotide, and Mg^{2+} (not shown).

Discussion

Ryanodine specifically interacts with the ligand-gated Ca^{2+} release channel that is localized at the terminal cisternae of striated muscle SR (15, 29). Characterization of the binding of [^{3}H]ryanodine has demonstrated the sensitivity of the alkaloid binding site to a large number of physiologically and pharmacologically relevant chemical agents (14, 17, 18). The number of interacting binding sites for ryanodine on the channel protein complex and their possible allosteric interaction have, until recently, been unclear. [^{3}H]Ryanodine binding sites having very low affinity (K_d ~3–5 μM) have been detected in both skeletal and cardiac SR, when assayed under high salt conditions (1 M KCl or NaCl) (14, 22). High salt has been shown to alter both the kinetics of ryanodine binding and the Ca^{2+}-transport properties of the release channel in isolated SR (8, 28, 30). As was pointed out in the Introduction, there is a discrepancy in the literature concerning the cooperative nature of the binding of ryanodine to the SR Ca^{2+} release channel complex (14, 22, 30).

Four heterogeneous sites for ryanodine on the SR Ca^{2+} release channel. Detailed investigation of equilibrium and kinetic binding parameters with isolated skeletal and cardiac SR, utilizing several "discriminating" concentrations of [^{3}H]ryanodine, strongly suggests the existence of more than three binding sites on the Ca^{2+} release channel complex (Table 1). Equilibrium binding assays show multiple binding sites for ryanodine, with the highest affinity being 4.6 nM in skeletal and 1.5 nM in cardiac SR. The Hill coefficient for the high affinity site is not significantly different from 1. This is not surprising, because the Hill plot measured at a ligand concentration that results in occupancy of 50–75% of B_{max} is significantly less than 1, whereas at very low and very high ligand concentrations n_H will approach 1 (31) when the binding curve reflects only one site. Binding curves with 0.25 nM to 2 μM [^{3}H]ryanodine (which titrates at least 75% of all available sites) give Hill coefficients significantly less than 1 (n_H = 0.55 and 0.63 in Table 1). Two distinct experimental approaches have been undertaken to demonstrate the presence of lower affinity sites. First, equilibrium binding of 0.5–1 nM [^{3}H]ryanodine was

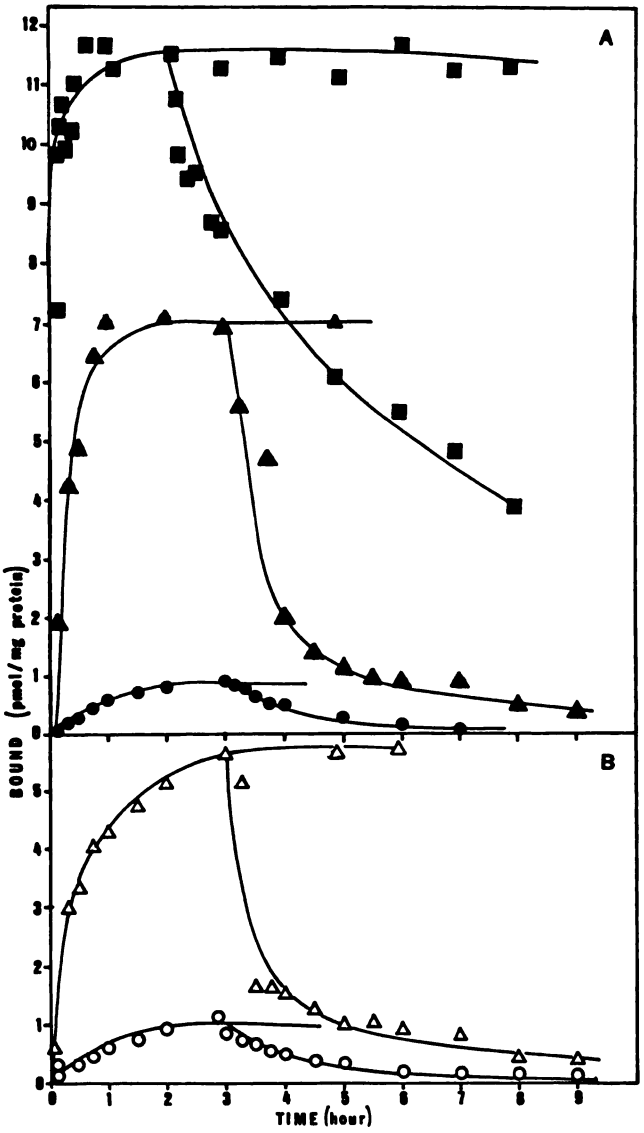

Fig. 6. Association of 1 (●, ○), 50 (▲, △), or 1000 (■) nM [^{3}H]ryanodine to 30 μg of skeletal (A) or cardiac (B) SR and dissociation by 100-fold dilution of the assay medium after equilibrium binding of ryanodine. Binding of [^{3}H]ryanodine was measured as described in Materials and Methods. Data shown are the average of two independent experiments performed in duplicate. Standard error was less than 5%. A, k_{obs} values for the binding of 1, 50, and 1000 nM ryanodine are 0.02575, 0.06223, and 0.5921 min^{-1} values, respectively, and k_{-1} values are 0.0129, 0.0182, and 0.00286 min^{-1}, respectively. B, k_{obs} values for the binding of 1 and 50 nM ryanodine are 0.02375 and 0.0637 min^{-1}, respectively, and k_{-1} values are 0.0077 and 0.0173 min^{-1}, respectively.

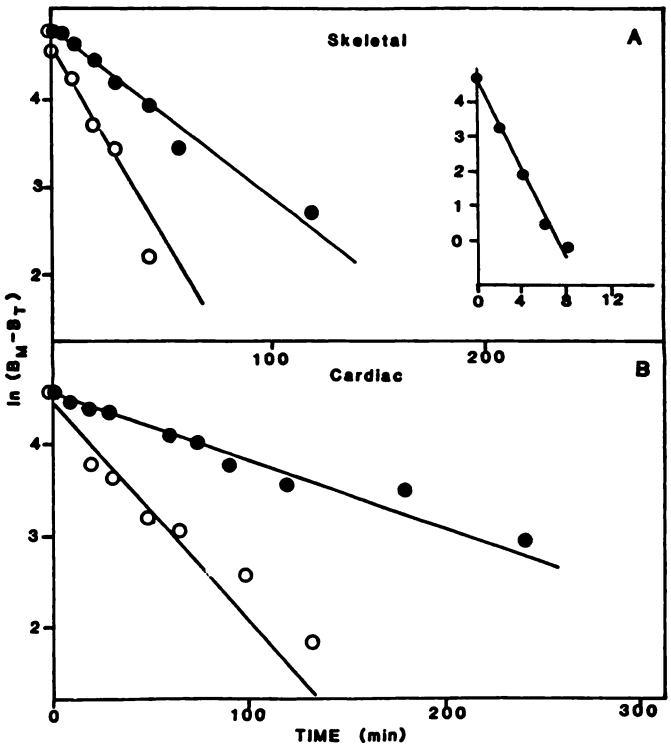

Fig. 7. Association curves of the binding of 1 (●), 50 (○), or 1000 (*inset*) nM [^{3}H]ryanodine to 30 μg of skeletal SR (A) and of 1 (●) or 50 (○) nM [^{3}H]ryanodine to cardiac SR (B). Data shown are from single representative experiments performed in duplicate. For skeletal SR, k_{obs} values are 0.01846, 0.0424, and 0.592 min^{-1} at 1, 50, and 1000 nM [^{3}H] ryanodine, respectively, and, for cardiac SR, k_{obs} values are 0.00774 and 0.0278 min^{-1} at 1 and 50 nM [^{3}H]ryanodine, respectively. B_M, maximal specific binding; B_T, specific binding at time t.

assessed in the presence of varying concentrations (0.5–500 nM) of unlabeled ryanodine. Second, equilibrium binding of 15, 50, or 300 nM [^{3}H]ryanodine, concentrations that saturate the high affinity sites, was assessed with varying concentrations (20 nM to 10 μM) of unlabeled ryanodine. Both approaches demonstrate the existence of three additional binding sites having lower affinities for [^{3}H]ryanodine (Table 1). The underlying causes of nonlinear Scatchard plots may be the result of (32) 1) ligand heterogeneity (labeled and unlabeled ryanodine used in the present studies exceeded 98% purity), 2) ligand-ligand interaction (unlikely because ryanodine is a neutral alkaloid with high solubility in aqueous medium), 3) two-step reaction kinetics with ternary complex formation (kinetic analysis of association of [^{3}H]ryanodine with its receptor clearly obeys one-step bimolecular kinetics, as demonstrated in Fig. 7), 4) incorrect definition of specific binding (which is avoided by subtraction of the binding at a 100-fold excess of the unlabeled ligand as nonspecific binding in every experiment), 5) multiple receptor subtypes, or 6) negative cooperative site-site interaction. The latter two options are possible for the binding of ryanodine. However there are five lines of evidence in favor of the negative cooperativity. 1) With both tissues, discrimination of sites with decreased affinity for ryanodine gives progressively lower Hill coefficients (n_H values for K_{d_2}, K_{d_3}, and K_{d_4} are 0.7, 0.65, and 0.25, respectively), in strong support of negative cooperativity, as recently suggested by Lai *et al.* (14). 2) The estimated ratios of the high and low affinity sites in skeletal and cardiac muscle are 1:2.2 and 1:2.5, respectively, determined by equilibrium binding experiments, by dissociation of the equilibrium binding of 50 nM [^{3}H]ryanodine by 100-fold dilution in the assay medium (Fig. 8), or by Ca^{2+} release measurements activated by ryanodine (Fig. 3). These ratios are slightly different from 1:3 given by Lai *et al.* (14), which is accounted for by the fact that our experimental design can discriminate three of the four sites present that have affinities below 1 μM. Lack of accurate quantitation of the lowest affinity site appears to be a limitation of equilibrium binding studies under low salt conditions, especially because these experiments cannot accurately discriminate low affinity binding from nonspecific binding [that fraction of inhibitable binding that is insensitive to heat denaturation (data not

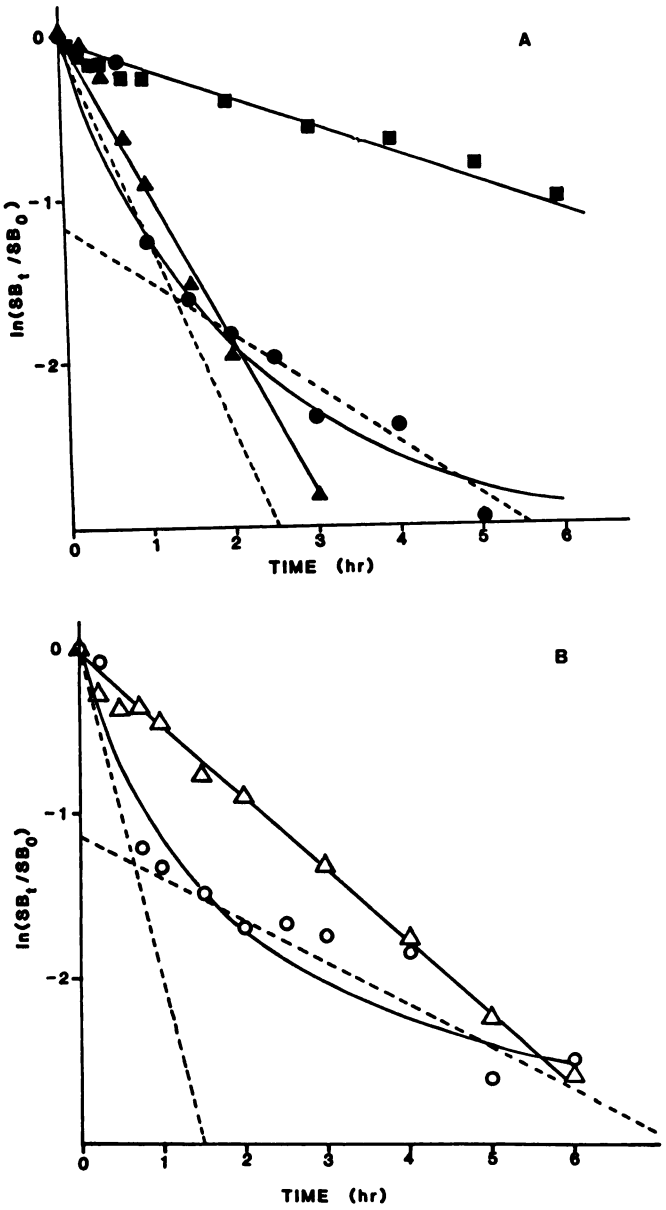

Fig. 8. Dissociation of 1 (▲, △), 50 (●, ○), and 1000 (■) nM [^{3}H]ryanodine from skeletal (A) and cardiac (B) SR by 100-fold dilution with the assay medium. At 1 nM [^{3}H]ryanodine, the corresponding k_{-1} values are 0.0167 min^{-1} for skeletal and 0.00776 min^{-1} for cardiac SR; the k_{-1} values at 50 nM [^{3}H]ryanodine are listed in Table 1 and k_{-1} at 1000 nM [^{3}H]ryanodine is 0.0028 min^{-1}. Dissociation was performed as described in Materials and Methods. Data are from single experiments performed in duplicate, which were repeated once with similar results. – – –, Linear fit for the fast and slow components of the dissociation after equilibrium binding with 50 nM [^{3}H]ryanodine, using the ENZFITTER program.

shown)]. 3) The existence of heterogeneous sites for ryanodine on the channel protein is supported by direct measurement of ryanodine-enhanced rates of Ca^{2+} release from SR actively loaded in the presence of ATP and a regenerating system (Fig. 3). The site having the lowest affinity for ryanodine in skeletal and cardiac SR can be determined (K_d = 2.4 ± 0.3 and 3.7 ± 0.2 μM, respectively) by measurement of the rate of Ca^{2+} release induced by different concentrations of ryanodine (Fig. 3). We demonstrate here that the binding properties of [^{3}H]ryanodine remain essentially unchanged in the complete transport buffer (Fig. 9), allowing valid correlation between receptor binding and Ca^{2+} release measurements. Under conditions promoting specific ryanodine binding sites having K_D values of 0.5–5 μM, a biphasic response of the channel is observed (discussed below), which suggests an allosteric link between high and low affinity sites. 4) Further evidence in support of allosteric negative cooperativity among four ryanodine binding sites comes from the analysis of [^{3}H]ryanodine binding kinetics. Determination of k_{-1} by dissociation of [^{3}H]ryanodine (5 nM in equilibrium with SR) by the addition of a micromolar excess of unlabeled ryanodine results in a biphasic rate of dissociation, with an extremely slow component (17) (Table 2). However, dissociation of [^{3}H]ryanodine (0.5 nM) from the high affinity sites by a 100-fold excess of unlabeled ryanodine (50 nM) yields linear rates that are quantitatively similar to rates obtained by addition of a 100-fold excess of assay medium. The association and dissociation rate constants (Figs. 7 and 8 and Tables 1 and 2) allow us to calculate the dissociation constants for the low and high affinity sites, which are in good agreement with the apparent dissociation constants derived from the equilibrium binding studies. The dissociation rate of 50 nM [^{3}H]ryanodine induced by a 100-fold dilution of assay medium is significantly faster than that of 1 nM [^{3}H]ryanodine. These kinetic results are consistent with an allosteric interaction among ryanodine binding sites that are negatively cooperative. This model predicts increased rates of dissociation with increasing concentrations of the dissociating ligand and excludes the possibility of four noninteracting binding sites. Measurement of association and dissociation (by 100-fold dilution with assay buffer) of 1 μM [^{3}H]ryanodine yields a calculated K_d that is not significantly different from the K_d measured at 1 nM [^{3}H]ryanodine (4.6 nM). This finding directly discounts the possibility of a full positively cooperative interaction at high concentrations of the alkaloid, as suggested by McGrew *et al.* (22). 5) Finally, pretreatment of SR with 1 μM ryanodine (which favors low affinity binding) results not only in the complete and irreversible inhibition of low affinity [^{3}H]ryanodine binding but also in significant inhibition of high affinity sites,[2] suggestive of an allosteric link among binding sites.

Sequential, time-dependent activation and inactivation of the Ca^{2+} release channel complex by ryanodine. Simple negative cooperativity cannot fully account for 1) the slowing of the second phase of dissociation at high ryanodine concentrations (Table 2) and 2) slowing of the rate of dissociation measured by 100- (Figs. 7 and 9) or 2000-fold (see text, above) dilution with the assay medium after equilibration of the SR with 1 μM [^{3}H]ryanodine. The action of high concentrations of ryanodine (Table 2), causing a sequential hastening and persistent delay in dissociation, may suggest a sequential, time-dependent, perhaps irreversible, alteration of the channel protein complex as a consequence of ryanodine binding. The existing discrepancy in the literature about the positive (22) or negative (14, 30) (present data) cooperative nature of the binding of ryanodine can be resolved by the suggestion that the effect of ryanodine on the initial (present data) and late phases (22) of the dissociation reveals different sequential mechanisms that result from the binding of ryanodine to its receptor sites. The possibility of a sequential mechanism was first suggested by Lai *et al.* (14), based on indirect observations. The present

[2] I. Zimanyi, E. Buck, J. Abramson, and I. Pessah. Irreversible Action of Ryanodine on Skeletal Muscle Sarcoplasmic Reticulum Channel. Manuscript in preparation.

TABLE 2

Comparison of dissociation rates of [^{3}H]ryanodine binding to skeletal and cardiac SR

Binding of [^{3}H]ryanodine was measured as described in Materials and Methods. Values are average of two independent determinations assayed in duplicate. Errors of the estimates were <10%.

Dissociating conditions	Skeletal				Cardiac			
	$t_{1/2}$	k_{-1}	k_{+1}	K_d	$t_{1/2}$	k_{-1}	k_{+1}	K_d
	min	min^{-1}	$nM^{-1}min^{-1}$	nM	min	min^{-1}	$nM^{-1}min^{-1}$	nM
100-fold excess of assay medium	53.6	0.0129	0.0090	1.43	89.1	0.0077	0.0071	1.08
25 nM Ryanodine	105.5	0.0066	0.0062	1.05	134.1	0.0052	0.0096	0.54
50 nM Ryanodine	104.5	0.0066	0.0062	1.06	109.0	0.0063	0.0085	0.74
10 μM Ryanodine[a]	101.9	0.0068	0.0060	1.13	90.0	0.0077	0.0071	1.08
10 μM Ryanodine[b]	302.4	0.0023	0.0105	0.22	401.0	0.0017	0.0131	0.13
200 nM RR[c]	132.6	0.0052	0.0076	0.68	290.0	0.0024	0.0124	0.19
1 μM RR	83.4	0.0083	0.0045	1.84	312.2	0.0022	0.0126	0.17
10 μM RR	104.2	0.0066	0.0062	1.06	305.5	0.0022	0.0126	0.17

[a] Taking the initial phase of dissociation only.
[b] Taking both the slow and initial phases of dissociation.
[c] RR, ruthenium red.

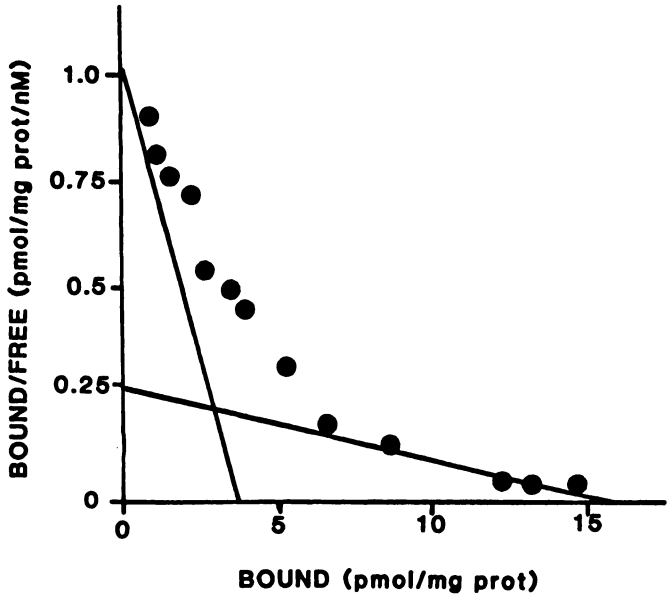

Fig. 9. Parameters of the equilibrium binding of [^{3}H]ryanodine to skeletal SR are not affected by pyrophosphate and antipyrylazo III. The binding of 0.5–500 nM [^{3}H]ryanodine to 30 μg of skeletal SR was performed in 1 ml of transport assay buffer consisting of 95 mM KCl, 20 mM K-MOPS, 7.5 mM sodium pyrophosphate, 250 μM antipyrylazo III, 1.5 mM MgATP, 25 μg/ml creatine phosphokinase, and 5 mM phosphocreatine, pH 7.0. Data shown are from a single experiment, performed in duplicate. K_d values for the high and low affinity sites are 3.76 and 55.9 nM, respectively, and the respective B_{max} values are 3.87 and 15.66 pmol/mg of protein.

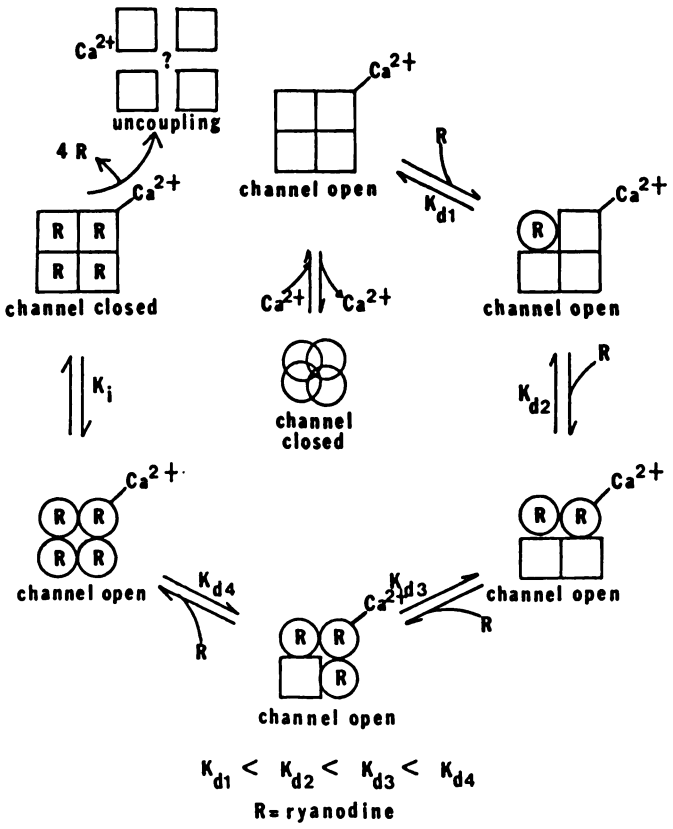

Fig. 10. Model of modulation of the Ca^{2+} release channel by ryanodine.

work, utilizing antipyrylazo III to rapidly monitor changes in extravesicular Ca^{2+} under active loading conditions and in the presence of the Ca^{2+}-complexing anion pyrophosphate, can clearly show the biphasic effect of ryanodine on the release of Ca^{2+} from the moment of the addition of the alkaloid to the SR of cardiac or skeletal muscle. The presence of pyrophosphate, which readily permeates SR, permits rapid loading of SR membrane vesicles with levels of Ca^{2+} that are not possible in its absence, while allowing slower depletion of the accumulated Ca^{2+} during the subsequent phase of rapid Ca^{2+} release (7). Because net transport of Ca^{2+} across SR vesicles can be accurately monitored in real time and reflects a balance between pump protein-mediated uptake and release through the release channel, the assay allows careful control of important parameters, including the amount of Ca^{2+} with which the vesicles are loaded and the extravesicular Ca^{2+} concentration at the time of drug-induced Ca^{2+} release, factors that have a significant influence on the initial rates of Ca^{2+} release. Further, Palade (10, 11) has demonstrated that, in the presence of pyrophosphate, rapid rates of Ca^{2+} release can be accurately measured and the SR Ca^{2+} release channel maintains its sensitivity to pharmacological agents known to influence its activity. The higher sensitivity of cardiac SR to Ca^{2+}-induced Ca^{2+} release is also quantitatively [if one considers the free Ca^{2+} attained in this study to be approximately one tenth of the total Ca^{2+} (10)] and qualitatively consistent with previous studies with isolated

SR and with skinned muscle fibers and could reflect the relevance of this mechanism in excitation-contraction coupling in cardiac muscle (33). Utilizing this technique, we can show the concentration-dependent activation and inactivation by ryanodine of the release of Ca^{2+} in both cardiac and skeletal SR preparations (Fig. 4), which directly support our receptor binding data and data on the action of ryanodine on single Ca^{2+} release channels, reconstituted into lipid bilayers, reported by Lai *et al.* (14).

Putting the transport and the receptor binding data together, we propose an alternative model (scheme in Fig. 10), whereby four negatively cooperative sites on the Ca^{2+} release channel protein allosterically modulate ryanodine binding and are coupled to sequential activation and inactivation of the Ca^{2+} release channel.

In the presence of low (<1 μM) Ca^{2+} concentrations, the four binding sites are in a low affinity conformation (characterized by slow rates of association) (17) and the channel is nonconducting (Fig. 10, *overlapping circles*). Micromolar Ca^{2+} induces a concerted transition to the high affinity ryanodine receptor state and a conducting channel (Fig. 10, *squares*).

The model stresses two important new findings regarding the interaction of ryanodine with its receptor. First, ryanodine binds to four sites on the oligomeric channel complex, which allosterically interact in a negatively cooperative manner with decreasing affinities (K_{d_1} = 1–3 nM, K_{d_2} = 30–50 nM, K_{d_3} = 500–800 nM, and K_{d_4} = 2000–4000 nM). Second, binding of ryanodine to its receptor activates the Ca^{2+} release channel in a concentration-dependent and saturable manner, in the range of 20 nM to 1 mM, and produces a kinetically limited and sequential inactivation of the Ca^{2+} channel, with the concomitant attainment of full negative cooperativity. The results presented also suggest that driving the complex toward full negative cooperativity with high concentrations of ryanodine promotes a long-lived conformational state in which ryanodine is physically occluded and hindered from free diffusion from its binding site.

Acknowledgments

The authors would like to thank Mary J. Schiedt for her excellent technical assistance.

References

1. Kirino, Y., M. Osakabe, and H. Shimizu. Ca^{2+}-induced Ca^{2+} release from fragmented sarcoplasmic reticulum: Ca^{2+}-dependent passive Ca^{2+} efflux. *J. Biochem.* **94**:1111–1118 (1983).
2. Nagasaki, K., and M. Kasai. Channel selectivity and gating specificity of calcium-induced calcium release channel in isolated sarcoplasmic reticulum. *J. Biochem.* **96**:1769–1775 (1984).
3. Kim, D. H., S. T. Ohnishi, and N. Ikemoto. Kinetic studies of calcium release from sarcoplasmic reticulum *in vitro*. *J. Biol. Chem.* **258**:9662–9668 (1983).
4. Meissner, G. Ryanodine activation and inhibition of the Ca^{2+} release channel of sarcoplasmic reticulum. *J. Biol. Chem.* **261**:6300–6306 (1986).
5. Meissner, G., and J. S. Henderson. Rapid calcium release from cardiac sarcoplasmic reticulum vesicles is dependent on Ca^{2+} and is modulated by Mg^{2+}, adenine nucleotide, and calmodulin. *J. Biol. Chem.* **262**:3065–3073 (1987).
6. Chamberlain, B. K., P. Volpe, and S. Fleischer. Calcium-induced calcium release from purified cardiac sarcoplasmic reticulum vesicles: general characteristics. *J. Biol. Chem.* **259**:7540–7546 (1984).
7. Palade, P. Drug-induced Ca^{2+} release from isolated sarcoplasmic reticulum. I. Use of pyrophosphate to study caffeine-induced Ca^{2+} release. *J. Biol. Chem.* **262**:6135–6141 (1987).
8. Hasselbach, W., and A. Migala. Activation and inhibition of the calcium gate of sarcoplasmic reticulum by high-affinity ryanodine binding. *FEBS Lett.* **221**:119–123 (1987).
9. Hasselbach, W., and A. Migala. Interaction of ryanodine with the calcium releasing system of sarcoplasmic reticulum vesicles. *Z. Naturforsch. Teil C. Biochem. Biophys. Biol. Virol.* **43**:140–148 (1987).
10. Palade, P. Releases involving Ca^{2+}-induced Ca^{2+} release channel. *J. Biol. Chem.* **262**:6142–6148 (1987).
11. Palade, P. Drug-induced Ca^{2+} release from isolated sarcoplasmic reticulum. III. Block of Ca^{2+}-induced Ca^{2+} release by organic polyamines. *J. Biol. Chem.* **262**:6149–6154 (1987).
12. Smith, J. S., T. Imagawa, J. Ma, M. Fill, K. P. Campbell, and R. Coronado. Purified ryanodine receptor from rabbit skeletal muscle is the calcium-release channel of the sarcoplasmic reticulum. *J. Gen. Physiol.* **92**:1–26 (1988).
13. Fill, M., and R. Coronado. Ryanodine receptor channel of sarcoplasmic reticulum. *Trends Neurosci.* **11**:453–457 (1988).
14. Lai, F. A., M. Misra, L. Xy, H. A. Smith, and G. Meissner. The ryanodine receptor-Ca^{2+} release channel complex of skeletal muscle sarcoplasmic reticulum. *J. Biol. Chem.* **264**:16776–16785 (1989).
15. Pessah, I. N., A. L. Waterhouse, and J. E. Casida. The calcium-ryanodine receptor complex of skeletal and cardiac muscle. *Biochem. Biophys. Res. Commun.* **128**:449–456 (1985).
16. Pessah, I. N., A. O. Francini, D. J. Scales, A. L. Waterhouse, and J. E. Casida. Calcium-ryanodine receptor complex: solubilization and partial characterization from skeletal muscle junctional sarcoplasmic reticulum. *J. Biol. Chem.* **261**:8643–8648 (1986).
17. Pessah, I. N., R. A. Stambuk, and J. E. Casida. Ca^{2+}-activated ryanodine binding: mechanisms of sensitivity and intensity modulation by Mg^{2+}, caffeine, and adenine nucleotides. *Mol. Pharmacol.* **31**:232–238 (1987).
18. Imagawa, T., J. S. Smith, R. Coronado, and K. P. Campbell. Purified ryanodine receptor from skeletal muscle sarcoplasmic reticulum is the Ca^{2+}-permeable pore of the calcium release channel. *J. Biol. Chem.* **262**:16636–16643 (1987).
19. Hymel, L., H. Schindler, M. Inui, and S. Fleischer. Reconstitution of purified cardiac muscle calcium release channel (ryanodine receptor) in planar bilayers. *Biochem. Biophys. Res. Commun.* **152**:308–314 (1988).
20. Inui, M., A. Saito, and S. Fleischer. Isolation of the ryanodine receptor from cardiac sarcoplasmic reticulum and identity with the feet structures. *J. Biol. Chem.* **262**:15637–15642 (1987).
21. Michalak, M., P. Dupraz, and V. Shoshan-Barmatz. Ryanodine binding to sarcoplasmic reticulum membranes: comparison between cardiac and skeletal muscle. *Biochim. Biophys. Acta* **939**:587–594 (1988).
22. McGrew, S. G., C. Wolleben, P. Siegl, M. Inui, and S. Fleischer. Positive cooperativity of ryanodine binding to the calcium release channel of sarcoplasmic reticulum of heart and skeletal muscle. *Biochemistry* **28**:1686–1691 (1989).
23. Saito, A., S. Seiler, A. Chu, and S. Fleischer. Preparation and morphology of sarcoplasmic reticulum terminal cisternae from rabbit skeletal muscle. *J. Cell Biol.* **99**:875–885 (1984).
24. Pessah, I. N., E. L. Durie, M. J. Schiedt, and I. Zimanyi. Anthraquinone-sensitized Ca^{2+} release channel from rat cardiac sarcoplasmic reticulum: possible receptor-mediated mechanism of doxorubicin cardiomyopathy. *Mol. Pharmacol.* **37**:503–514 (1990).
25. Harris, R. N., and J. H. Doroshow. Effect of doxorubicin-enhanced hydrogen peroxide and hydroxyl radical formation on calcium sequestration by cardiac sarcoplasmic reticulum. *Biochem. Biophys. Res. Commun.* **130**:739–745 (1985).
26. Lowry, O. H., N. J. Rosebrough, A. L. Farr, and R. J. Randall. Protein measurement with the Folin phenol reagent. *J. Biol. Chem.* **193**:265–275 (1951).
27. Bennett, J. P. Jr. Methods in binding studies, in *Neurotransmitter Receptor Binding* (H. I. Yamamura, S. J. Enna, and M. J. Kuhar, eds.). Raven Press, New York, 57–90 (1978).
28. Zimanyi, I., and I. N. Pessah. Comparison of [^{3}H]ryanodine receptors and Ca^{2+} release from rat cardiac and rabbit skeletal muscle sarcoplasmic reticulum. *J. Pharmacol. Exp. Ther.* **256**:938–946 (1991).
29. Fleischer, S., E. M. Ogunbunmi, M. C. Dixon, and A. M. Fleer. Localization of Ca^{2+} release channels with ryanodine in junctional terminal cisternae of sarcoplasmic reticulum of fast skeletal muscle. *Proc. Natl. Acad. Sci. USA* **82**:7256–7259 (1985).
30. Chu, A., M. Diaz-Munoz, M. J. Hawkes, K. Brush, and S. L. Hamilton. Ryanodine as a probe for the functional state of the skeletal muscle sarcoplasmic reticulum calcium release channel. *Mol. Pharmacol.* **37**:735–741 (1990).
31. Segel, I. H. *Enzyme Kinetics, Behavior and Analysis of Rapid Equilibrium and Steady State Enzyme Systems.* John Wiley & Sons, New York, 377–381 (1975).
32. Molinoff, P. B., B. B. Wolfe, and G. A. Weiland. Quantitative analysis of drug-receptor interactions. II. Determination of the properties of receptor subtypes. *Life Sci.* **29**:427–443 (1981).
33. Fleischer, S., and M. Inui. Biochemistry and biophysics of excitation-contraction coupling. *Annu. Rev. Biophys. Biophys. Chem.* **18**:333–364 (1989).

Send reprint requests to: Dr. Isaac N. Pessah, Department of Veterinary Pharmacology and Toxicology, University of California, Davis, CA 95616.